

# Mechanism of 1,2-Dichloroethane Dehydrochlorination on the Acid Sites of Oxide Catalysts as Studied by IR Spectroscopy

A. S. Shalygin<sup>a</sup>, L. V. Malysheva<sup>a</sup>, and E. A. Paukshtis<sup>a,b</sup>

<sup>a</sup>Boreskov Institute of Catalysis, Siberian Branch, Russian Academy of Sciences, Novosibirsk, 630090 Russia

<sup>b</sup>Novosibirsk State University, Novosibirsk, 630090 Russia

e-mail: shas@catalysis.ru

Received May 27, 2009

**Abstract**—The adsorption of 1,2-dichloroethane on zeolite HZSM-5 and  $\gamma$ -Al<sub>2</sub>O<sub>3</sub> at temperatures from 25 to 400°C was studied by Fourier transform IR spectroscopy. The forms of adsorbed 1,2-dichloroethane and the products of its conversion at the Brønsted and Lewis acid sites of catalysts were identified. The kinetics of 1,2-dichloroethane conversion on the surface of catalysts was studied by in situ Fourier transform IR spectroscopy. It was demonstrated that 1,2-dichloroethane was dehydrochlorinated at the Lewis sites of  $\gamma$ -Al<sub>2</sub>O<sub>3</sub> even at 100°C, whereas the reaction came into play at the Brønsted sites of zeolite HZSM-5 only at 200°C. It was found that, at the Lewis acid sites of catalysts, the resulting vinyl chloride underwent oligomerization with the intermediate formation of a dimer (1,3-dichloro-2-butene), whereas the formation of 1,3-dichloro-2-butene at the Brønsted sites of zeolite HZSM-5 was not observed. The mechanisms of 1,2-dichloroethane conversions at Lewis and Brønsted acid sites were proposed.

**DOI:** 10.1134/S0023158411020169

## INTRODUCTION

Vinyl chloride is a large-scale product of the chemical industry. To 98% of manufactured vinyl chloride is used for the production of polyvinyl chloride. Vinyl chloride is commercially manufactured by the gas-phase pyrolysis of 1,2-dichloroethane (DCE) at a pressure of 2–2.5 MPa and a temperature of 480–520°C. The selectivity of vinyl chloride formation was 98.5–98.7% at a DCE conversion of lower than 55% [1]. An increase in the conversion with temperature or contact time was accompanied by a considerable decrease in the selectivity. It was hypothesized that the use of catalysts makes it possible to decrease the reaction temperature and thereby to increase the process selectivity. Various systems, including zeolites, were studied in the catalytic dehydrochlorination of DCE [2]. It was found that all of the catalysts without exception rapidly deactivated in the course of reaction. However, the effects of the nature, strength, and concentration of acid sites on both activity in DCE dehydrochlorination and catalyst deactivation have not been studied systematically. There are a few publications devoted to the mechanism of this reaction. Uvarova et al. [2] hypothesized that the conversion of DCE into vinyl chloride occurred by a two-centered mechanism on an acid–base pair. It was found by IR spectroscopy that the dehydrochlorination of DCE on oxides was accompanied by the formation of acetaldehyde [3, 4]. In a study of the dehydrochlorination reaction of DCE on a series of binary oxide catalysts having different acid–base properties, the degrees of

participation of Brønsted and Lewis acid sites (BASs and LASs, respectively) in the conversion of DCE were determined and a hypothesis was proposed that the formation and subsequent transformations of 1,3-dichloro-2-butene are responsible for catalyst deactivation [5].

The aim of this work was to study the kinetics and mechanism of DCE conversion on zeolite HZSM-5 and aluminum oxide using in situ Fourier transform IR spectroscopy.

## EXPERIMENTAL

### Catalysts

Preparation and characterization procedures and the properties of  $\gamma$ -Al<sub>2</sub>O<sub>3</sub> were described elsewhere [5]. Zeolite HZSM-5, which was prepared in accordance with a published procedure [6], had the silicate module Si/Al = 47 and the degree of ion exchange of 96%. The procedures of measuring acid properties were described in a monograph [7]. Table 1 summarizes the specific surface areas and acid properties of the catalysts.

IR spectra were recorded on a FTIR 8300 spectrometer from Shimadzu over a range of 400–6000  $\text{cm}^{-1}$  with a resolution of 4  $\text{cm}^{-1}$ ; the number of scans was varied from 10 to 100 depending on a time interval between the measurements of spectra.

**Table 1.** Acid properties of catalysts

Catalyst	$S_{sp}$ , $\text{m}^2/\text{g}$	BAS		LAS	
		strength	concentration	strength	concentration
		PA, $\text{kJ/mol}$	$N_{\text{H}^+}$ , $\mu\text{mol/g}$	$Q_{\text{CO}}$ , $\text{kJ/mol}$	$N_{\text{CO}}$ , $\mu\text{mol/g}$
HZSM-5	555	1180	300	36	64
				33	18
$\gamma\text{-Al}_2\text{O}_3$	200	1410	60	55	36
				34	350

*Study of the Adsorption of DCE and Its Conversion at Various Temperatures*

A sample prepared as a pellet ( $15\text{--}35 \text{ mg/cm}^3$ ) was evacuated in a cell at  $500^\circ\text{C}$  for 1 h and cooled to room temperature, and the IR spectrum was recorded. The adsorption of previously distilled DCE (reagent grade) was performed at room temperature. The reagent dose, which was equal to the number of acid sites in the sample ( $\sim 350 \mu\text{mol/g}$ ), was introduced into the cell with a microsyringe. Thereafter, the pellet was kept at  $100^\circ\text{C}$  for 15 min and then cooled to room temperature. Next, the sample was consecutively heated at  $200$ ,  $300$ , and  $400^\circ\text{C}$ . The IR spectra were measured at room temperature after injecting DCE and after each heating. In the course of heating, converted substances were not removed from the cell; therefore, they were repeatedly adsorbed on the surface upon cooling the pellet.

The absorption bands of DCE, vinyl chloride, 1,3-dichlorobutene, and acetaldehyde were attributed based on published data [3, 4, 8, 9]. The concentrations of hydrogen chloride, acetaldehyde, and carbonate-carboxylates were calculated from integrated band intensities with the use of integrated absorption coefficients, which were determined in this work. The integrated absorption coefficient for a band due to the CO stretching vibrations ( $\nu(\text{CO}) = 1670\text{--}1743 \text{ cm}^{-1}$ ) of acetaldehyde was determined from experiments on the dosed adsorption of acetone, formaldehyde, and acetaldehyde on zeolite HZSM-5 and Aerosil at room temperature. The dosing was performed by injecting the test substance into a special small IR cell ( $30 \text{ cm}^3$ ) with a gas or liquid microsyringe. The surface area of cell walls with consideration for roughness was less than 1% of the total surface area of the sample; this allowed us to ignore the adsorption of the substance on the cell. The integrated absorption coefficient for a band due to the antisymmetric stretching vibrations of carbonate-carboxylate structures ( $\nu(\text{COO}^-) = 1470\text{--}1650 \text{ cm}^{-1}$ ) was determined from the IR spectra of the acetate salts of alkali and alkaline earth metals in KBr. The coefficients for the entire groups of compounds were  $\sim 10 \pm 2 \text{ cm}/\mu\text{mol}$ . The integrated absorption coefficient for a band due to HCl at  $2800 \text{ cm}^{-1}$ , which was determined from the IR spectra of gas mixtures of

HCl in argon, was  $0.046 \text{ cm}/\mu\text{mol}$ . The amount of hydroxyl groups was calculated from their integrated intensities with the use of corresponding published integrated absorption coefficients [7].

*Kinetic Study of DCE Conversion*

A sample as a pellet was placed in an IR reactor cell, evacuated at  $500^\circ\text{C}$  for 1 h, and cooled to reaction temperature; then, the IR spectrum was recorded. Next,  $1 \mu\text{l}$  ( $12.5 \mu\text{mol}$ ) of DCE was injected and the recording of IR spectra was started. The spectra of the sample were measured within the first minute at 15-s regular intervals and then at 30-s regular intervals; next, the interval between the measurements of the spectra was gradually increased to 10 min. The total measurement time was 50–60 min. The kinetics of DCE conversion on the surface was studied at temperatures at which a noticeable conversion of DCE was observed: at  $200$  and  $100^\circ\text{C}$  on zeolite HZSM-5 and  $\gamma\text{-Al}_2\text{O}_3$ , respectively. The concentrations of the observed substances for which integrated absorption coefficients are known are given in percents on an injected DCE basis ( $N/N_{\text{DCE}}^{\text{init}}$ ). The concentrations of substances for which integrated absorption coefficients are unknown are given in percent of the maximum band intensity ( $I/I_{\text{max}}$ ). Note that, at  $200^\circ\text{C}$ , the adsorption of DCE on zeolite was as low as a small fraction of its amount added to the cell because the maximum band intensity at  $1433 \text{ cm}^{-1}$  was only 10–20% of the intensity of this band measured at room temperature at the same amount of injected DCE. Adsorption at this coverage was approximately described by the Henry equation. A comparison between band intensities for a gas phase and an adsorbed state indicates that, in a cell with an optical path length of 1 cm, the intensities of bands due to gaseous products other than HCl ( $2800 \text{ cm}^{-1}$ ) were extremely low against the background of absorption bands due to adsorbed substances. In this case, the measured spectra can be attributed to only adsorbed substances. Therefore, the band intensities of adsorbed DCE at  $200^\circ\text{C}$  were proportional to the total amount of DCE in the cell in accordance with the

**Table 2.** Attribution of absorption bands in the IR spectra of DCE and the reaction products of DCE dehydrochlorination

Absorption band (surface complex)	Absorption bands of the reagent and reaction products (gaseous (g) and liquid (l))					
	adsorbed on catalysts		1,2-dichloro- ethane	vinyl chlo- ride (g)	1,3-dichloro- 2-butene (g)	acetaldehyde (g)
	HZSM-5	Al <sub>2</sub> O <sub>3</sub>				
δ (HCCI) (1,2-dichloroethane)	Beyond the examinable spectral range	1238	1233 (g, l)	—	1250	—
δ (CCH) (1,2-dichloroethane)		1288	1284 (g, l)	1279	—	—
v(CC) + δ(CCH) (1,2-dichloroethane)	1316	1315	1313 (g, l)	—	—	—
δ (CH <sub>3</sub> ) (acetaldehyde)	1364	1358	—	—	—	1352
δ (CH <sub>2</sub> ) (vinyl chloride)	—	1372	—	1372	—	—
δ (CH <sub>3</sub> ) (acetaldehyde)	—	1400	—	—	1442	1400
		1422				1420
δ (CH <sub>2</sub> Cl) (1,2-dichloroethane)	1433	1431	1429 (l)	—	—	—
	1455	1453	1450 (g, l)	—	—	—
v (COO <sup>−</sup> ) (surface carbonate— carboxylate groups) [4]	—	1470	—	—	—	—
	—	1570	—	—	—	—
v (C=C) (oligomers)	1600–1607	1590	—	—	—	—
v (C=C) (vinyl chloride)	1635	1635	—	1620	—	—
v (C=C) (adsorbed dimer)	1664	1652	—	—	1650	—
v (C=O) (coordinated acetalde- hyde) [3]	1686	1684	—	—	—	—
v (C=O) (acetaldehyde)	1712	—	—	—	—	1743 (s)
v (CH) (CH <sub>2</sub> - and CH <sub>3</sub> -groups in various compounds)	—	—	—	—	—	2822
	2854	2850	2845 (l)	—	—	—
	2884	2881	2875 (l)	2875	2892	—
	—	2940	2957 (g)	—	2942	—
	2964	2966	—	2950	—	2967
	2975	—	2983 (g)	2970	2975	—
	—	3010	3005 (g)	—	—	3005 (traces)
v (=CH <sub>2</sub> ) (vinyl chloride)	3030	3027	—	—	3042	—
v (=CH—) (1,3-dichloro-2- butene)	3095	—	—	3107	—	—

Henry equation. Hence, it follows that the ratio  $(I_{\text{DCE}}^{\text{max}} - I_{\text{DCE}}^{\text{curr}}) / I_{\text{DCE}}^{\text{max}}$ , where  $I_{\text{DCE}}^{\text{max}}$  and  $I_{\text{DCE}}^{\text{curr}}$  are the maximum and current intensities of the IR absorption band of DCE, respectively, is approximately equal to the conversion of DCE. In individual experiments performed at room temperature, we found that adsorption equilibrium was rapidly established for no longer than 15 s. On aluminum oxide at 100°C, injected DCE almost entirely occurred on the surface.

## RESULTS AND DISCUSSION

Table 2 summarizes the attribution of absorption bands due to gaseous and liquid DCE, DCE adsorbed on zeolite HZSM-5 and  $\gamma$ -Al<sub>2</sub>O<sub>3</sub>, and DCE conversion products. The spectrum of adsorbed DCE is similar to the spectrum of a liquid, which is typical of molecules weakly bound to the surface. Adsorbed DCE was identified against the background of other surface compounds based on the appearance of bands at 1313, 1429, 1450, and 2845  $\text{cm}^{-1}$ ; vinyl chloride was identi-

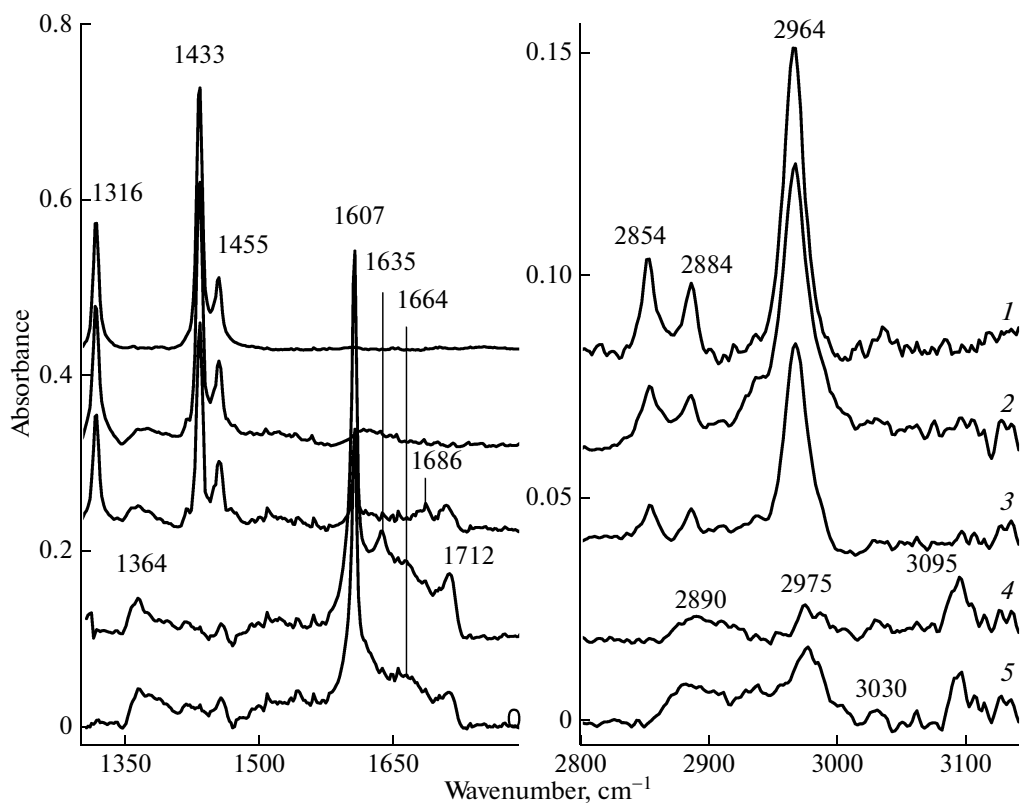


Fig. 1. IR spectra of DCE adsorbed on zeolite HZSM-5 at (1) 25, (2) 100, (3) 200, (4) 300, and (5) 400°C.

fied based on absorption bands at 1372, 1620–1635, and 3095–3107  $\text{cm}^{-1}$ ; 1,3-dichloro-2-butene was identified using absorption bands at 1650 and 3042  $\text{cm}^{-1}$ , and acetaldehyde was identified based on absorption bands at 1352, 1686, and 1712  $\text{cm}^{-1}$ . Absorption bands observed at 1460–1470 and 1570  $\text{cm}^{-1}$  in the spectra are characteristic of  $\nu(\text{COO}^-)$  of surface carbonate–carboxylate groups [4, 9], whereas bands in the range of 1590–1607  $\text{cm}^{-1}$  are characteristic of the vibrations of the  $-\text{C}=\text{C}-$  fragment in oligomer structures [9].

#### Zeolite HZSM-5

Unfortunately, the nature of adsorption sites cannot be determined from the spectra of DCE. This is due to the fact that no considerable changes in the electronic structure of DCE occur upon the formation of DCE complexes with LASs and BASs. The complexes of DCE with BASs were identified based on an analysis of changes in the spectra of OH groups. A shift in the band due to bridging OH groups from 3614 to 3280  $\text{cm}^{-1}$  was observed upon the adsorption of DCE on zeolite HZSM-5 at room temperature. The amount of adsorbed DCE was approximately the same as the amount of OH groups. This fact suggests the interaction of DCE with acid OH groups to form hydrogen-bonded complexes.

The IR spectra of DCE adsorbed on zeolite HZSM-5 at room temperature and 100°C (Fig. 1) coincide with the spectra of liquid DCE. Hence, it follows that no changes in DCE were observed. After heating at 200°C, bands due to vinyl chloride (1635 and 3095  $\text{cm}^{-1}$ ) appeared in the spectrum, whereas absorption bands characteristic of acetaldehyde (1686 and 1712  $\text{cm}^{-1}$ ), 1,3-dichloro-2-butene (1664 and 3030  $\text{cm}^{-1}$ ), and oligomers (1607  $\text{cm}^{-1}$ ) appeared at 300°C. Heating to 400°C resulted in a decrease in the intensities of absorption bands due to acetaldehyde and vinyl chloride; in this case, absorption bands characteristic of 1,3-dichloro-2-butene and oligomer structures were observed in the spectra.

Figure 2 shows changes in the concentrations of adsorbed DCE and its conversion products on zeolite HZSM-5 with time. The surface concentration of DCE reached a maximum in the first 15 s (curve 1). Next, it rapidly decreased to 40% of a maximum value and then slowly decreased to almost zero. Adsorbed vinyl chloride (curve 2) was detected only 10–12 min after the injection of DCE; then, a slow increase in its concentration with time was observed. The accumulation of oligomers (curve 3) occurred in a complicated manner: in the first minute, adsorbed oligomers were absent at the surface; starting with the second minute, their concentration dramatically increased and reached a constant value by 12 min. Thereafter, the

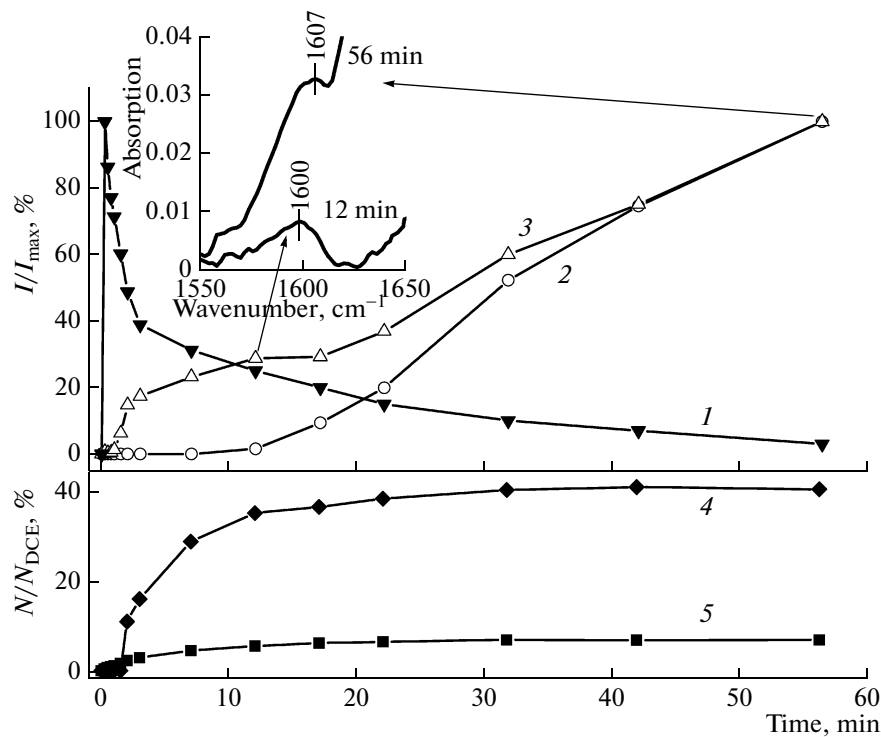


Fig. 2. The time dependence of the relative concentrations of adsorbed DCE and its conversion products on the surface of zeolite HZSM-5 at 200°C: (1) DCE ( $1433\text{ cm}^{-1}$ ), (2) vinyl chloride ( $1635\text{ cm}^{-1}$ ), (3) diene-type oligomers ( $1600\text{ cm}^{-1}$ ), (4) HCl ( $2800\text{ cm}^{-1}$ ), and (5) acetaldehyde ( $1712\text{ cm}^{-1}$ ). Insert: IR absorption bands due to oligomers after 12 and 56 min.

stage of a slow growth in the amount of oligomers on the surface came into play; it occurred simultaneously with an increase in the concentration of adsorbed vinyl chloride. At this stage, a shift in the band due to oligomers from  $1600$  to  $1607\text{ cm}^{-1}$  was observed. This was likely due to the occurrence of two types of structurally different oligomers. A small fraction of 1,2-dichloroethane (<7%) was converted into acetaldehyde (curve 5). Acetaldehyde was formed immediately after the injection of DCE, and a maximum concentration was reached within 20 min. Hydrogen chloride did not immediately appear in a gas phase; it appeared only 1.5 min after the injection of the reagent (curve 4). Thus, HCl was completely absorbed by the catalyst within the first minutes, and then the rate of DCE conversion became approximately equal to the rate of HCl release (curves 1 and 4).

We estimated the rate constant of adsorption based on an observation that the adsorption of DCE on zeolite at room temperature occurred for no longer than 15 s. It is about  $10^{-1}\text{ s}^{-1}$ , which is much higher than the rate constants of other transformations. Consequently, the kinetics of DCE conversion into products is not limited by diffusion. The rate constants of DCE dehydrochlorination on the zeolite surface at 200°C were calculated assuming a first-order reaction for two portions of kinetic curve 1 (Fig. 2) to be  $5.7 \times 10^{-3}\text{ s}^{-1}$  over a range from 0.25 to 2 min and  $0.77 \times 10^{-3}\text{ s}^{-1}$  from 7

to 56 min. Hence, it is obvious that deactivation can occur due to the blocking of BASs by coke deposits, the blocking of LASs by coke, or the degradation of LASs by HCl released in the dehydrochlorination reaction.

The change of the Brønsted acidity in the course of DCE conversion was studied using the spectra of OH groups. Figure 3 shows the IR spectra in the OH group vibration range for the initial zeolite HZSM-5 (curve 1), and for the same zeolite 15 s, 7 min, and 56 min after DCE admission at 200°C (curves 2–4, respectively). Curves 5–8 in Fig. 3 illustrate the kinetics of variation of the OH band intensities. A band at  $3610\text{ cm}^{-1}$  belongs to the stretching vibrations of the OH groups of BASs. (A shift toward the low-frequency region from  $3614$  to  $3610\text{ cm}^{-1}$  with increasing temperature was a consequence of corresponding anharmonic vibrations.) Bands at  $3640$ – $3700\text{ cm}^{-1}$  were due to the vibrations of Al–OH groups bound to nonskeletal aluminum. A band at  $3740\text{ cm}^{-1}$  belongs to the terminal Si–OH groups of the zeolite.

Upon the injection of DCE (curves 2 and 3), the intensities of absorption bands due to Al–OH groups at  $3640$  and  $3700\text{ cm}^{-1}$  increased, whereas the intensity of a band due to OH groups at  $3610\text{ cm}^{-1}$  decreased. A band at  $3335\text{ cm}^{-1}$ , which appeared after DCE adsorption, belongs to bridging OH groups hydrogen bonded to DCE. The concentration of OH

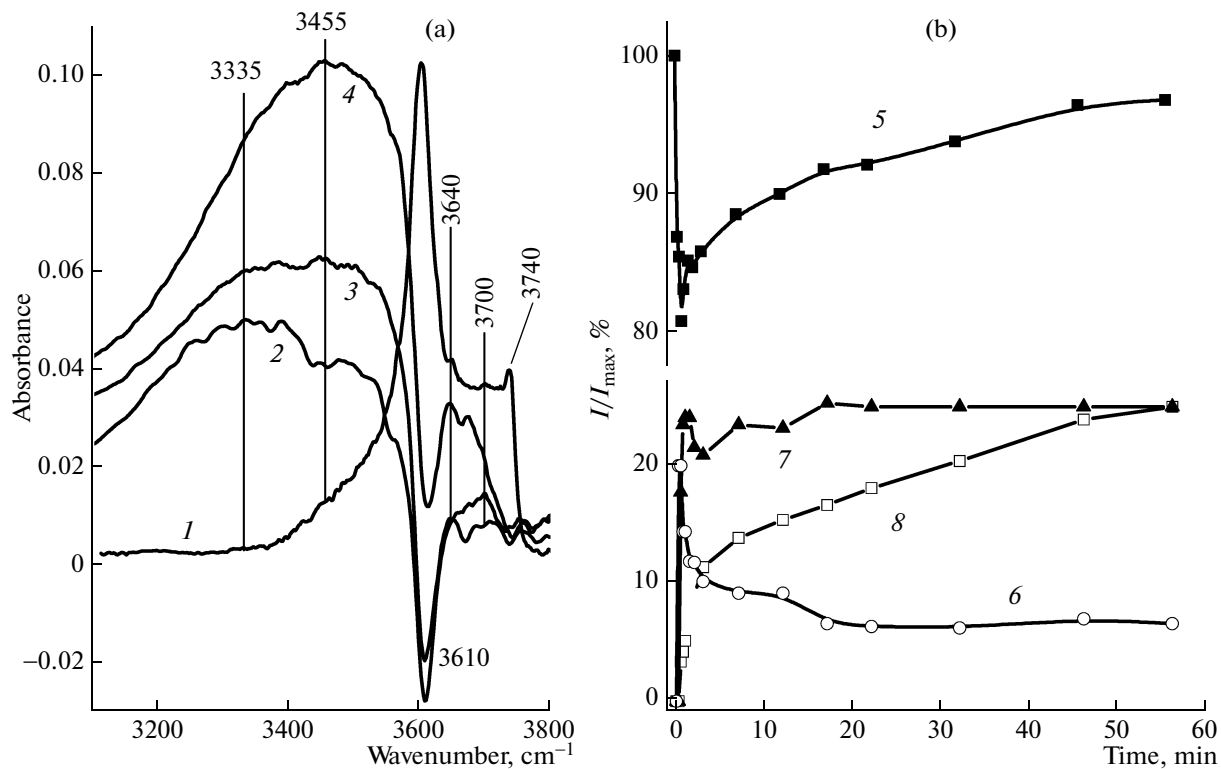


**Fig. 3.** Changes in the concentration of OH groups in zeolite HZSM-5 in the course of DCE conversion at 200°C. (a) IR spectra in the region of OH-group vibrations for (1) the initial zeolite (band intensities were decreased by a factor of 3) and (2) 0.25, (3) 7, and (4) 56 min after DCE injection. (b) The time dependence of the relative concentrations of OH groups in HZSM-5 corresponding to IR absorption bands at (5) 3610, (6) 3335, (7) 3700, and (8) 3455 cm<sup>-1</sup>.

groups characterized by an absorption band at 3610 cm<sup>-1</sup> (curve 5) decreased after the adsorption of DCE for 45 s to 80% on an initial basis; in this case, the concentration of hydrogen-bonded OH groups (3335 cm<sup>-1</sup>) (curve 6) reached a maximum within the same time interval. At the end of the experiment, the intensity of the band due to OH groups at 3610 cm<sup>-1</sup> (curve 5) increased from 80 to 95%, and the absorption band at 3335 cm<sup>-1</sup> due to hydrogen-bonded OH groups (curve 6) (normalized to a maximum band intensity at 3610 cm<sup>-1</sup>) decreased from 20 to 5%. As a result of the interaction of HCl with AlO clusters that left the skeleton, which are responsible for the existence of LASs, isolated (3640, 3680, and 3700 cm<sup>-1</sup>) and hydrogen-bonded Al-OH groups (a band at 3455 cm<sup>-1</sup>) are formed. The band intensity at 3700 cm<sup>-1</sup> (curve 7) rapidly increased within the first minute after the injection of DCE and then remained unchanged. The band intensity at 3455 cm<sup>-1</sup> (curve 8) increased during the entire observation time. Curves 7 and 8, which reflect changes in the concentrations of isolated and hydrogen-bonded Al-OH groups, respectively, were normalized to the concentration of hydrogen chloride, ~50% of which was consumed for the formation of these groups. Because the major portion of BASs (OH groups; 3610 cm<sup>-1</sup>) remained free in the course of the reaction, we can assume on this basis

that deactivation due to the blocking of OH groups by oligomers was absent or it did not give a noticeable contribution to deactivation.

As noted above, the observed zeolite deactivation (Fig. 2, curve 1) can be due to either the accumulation of oligomers at LASs or the blocking of these sites because of their interaction with HCl.

At AlO clusters, the dehydrochlorination can occur in accordance with the reaction scheme  $DCE + AlOAl \rightarrow$  vinyl chloride + AlOH + AlCl, in which the LAS (Al) and basic site (O) pair participates. The interaction of HCl with AlO clusters changes an endothermic gas-phase reaction of DCE dehydrochlorination to an exothermic reaction. As shown in Fig. 3, at a 97% conversion of DCE, only 40% HCl occurred in a gas phase; that is, 57% HCl interacted with out-of-skeleton AlO clusters of the zeolite. In this case, in the first minutes, oligomers were almost absent at the surface, but deactivation occurred. Hence, we can hypothesize that the deactivation was due to the above reaction, as a result of which HCl blocked both LAS and basic site. On BASs, the dehydrochlorination reaction occurred with the release of HCl.

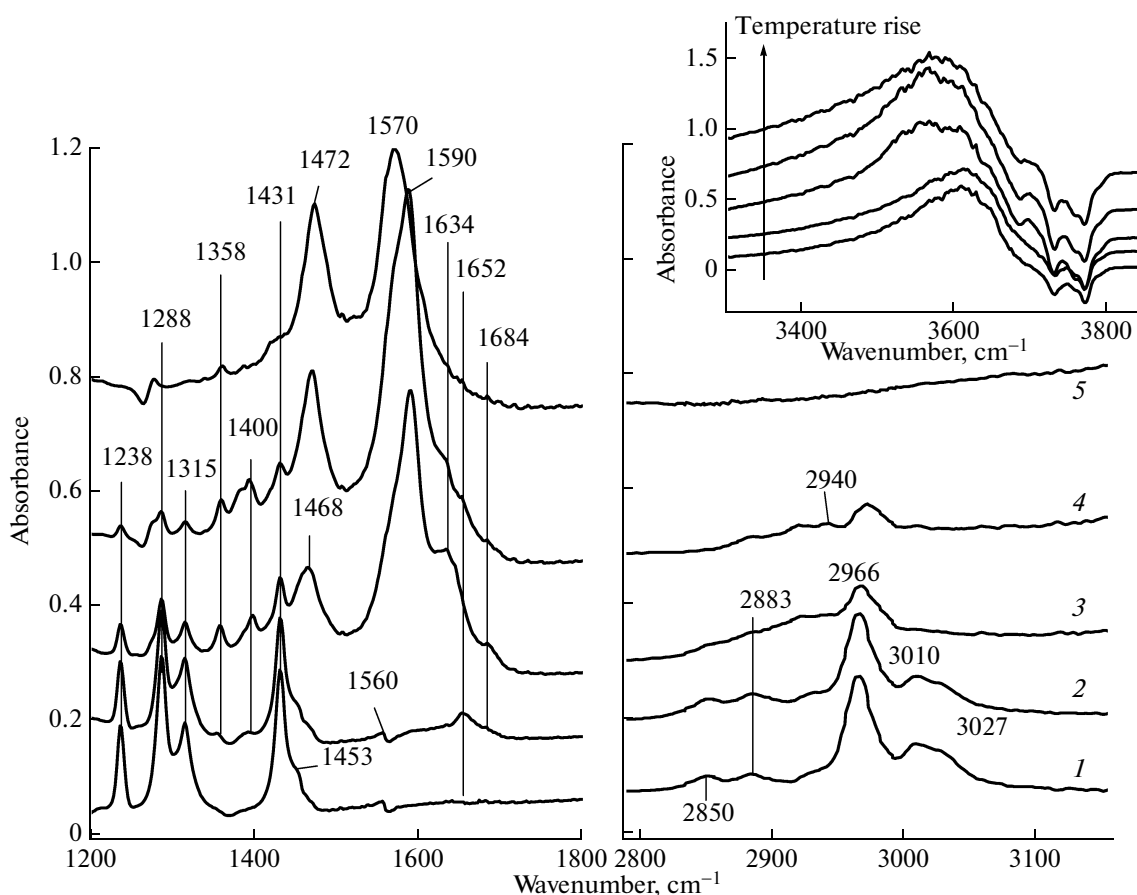
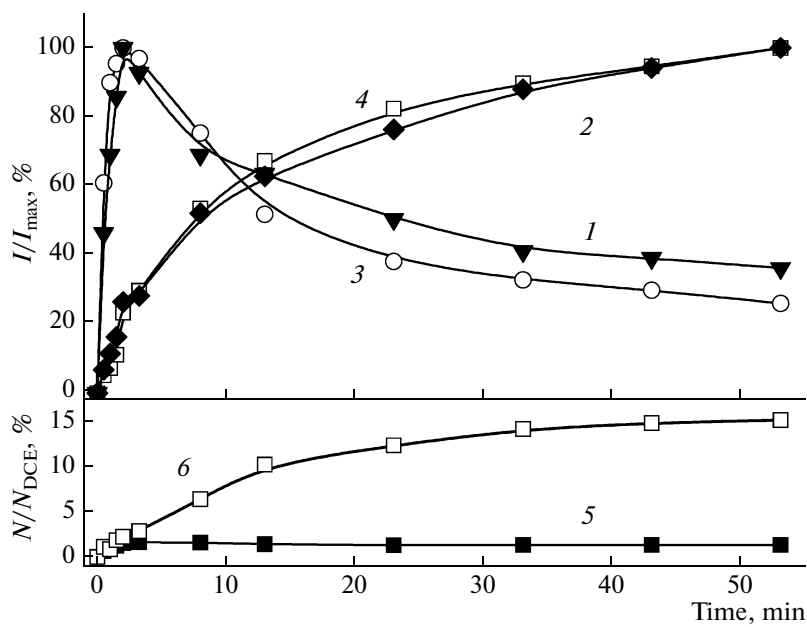


Fig. 4. IR spectra of DCE adsorbed on  $\gamma$ -Al<sub>2</sub>O<sub>3</sub> at (1) 25, (2) 100, (3) 200, (4) 300, and (5) 400°C.

The rate of deactivation can be estimated assuming that DCE is converted in accordance with the first-order equation  $w = -dC/dT = kC_{\text{site}}C_{\text{DCE}}$ , where  $k$  is the reaction rate constant, and  $C_{\text{site}}$  and  $C_{\text{DCE}}$  are the concentrations of sites and DCE, respectively. An analysis of the time dependence of  $w/C_{\text{DCE}}$  indicated that, at times longer than 7 min, the  $w/C_{\text{DCE}}$  ratio was almost constant; consequently, deactivation did not occur. Hence, we can conclude that dehydrochlorination at times longer than 7 min occurred on BASs. In a time interval of 30 s–7 min, the  $w/C_{\text{DCE}}$  ratio decreased from  $8.8 \times 10^{-3}$  to  $0.8 \times 10^{-3}$  s<sup>-1</sup> in accordance with an approximately exponential law. Thus, the rate constant of deactivation is approximately equal to the reaction rate constant of DCE conversion. The initial rate constant at LASs is  $8.8 \times 10^{-3}$  s<sup>-1</sup>, and the rate constant on BASs is  $0.77 \times 10^{-3}$  s<sup>-1</sup>. If we compare these constants with the number of sites, we found that the activity of a single medium-strength LAS ( $Q_{\text{CO}} = 35$  kJ/mol;  $N_{\text{H}^+} = 64$   $\mu\text{mol/g}$ ) is higher than the activity of a strong BAS (the BAS deprotonation energy (PA) is 1180 kJ/mol, and  $N_{\text{H}^+} = 300$   $\mu\text{mol/g}$ ) by a factor of 50.

#### Aluminum Oxide

Bands at 1652 and 3027 cm<sup>-1</sup>, which are characteristic of 1,3-dichloro-2-butene, appeared in the IR spectrum of DCE adsorbed on  $\gamma$ -Al<sub>2</sub>O<sub>3</sub> even at room temperature (Fig. 4). On heating to 100°C, bands at 1358, 1398, and 1684 cm<sup>-1</sup> due to acetaldehyde adsorbed at LASs additionally appeared. A shift in  $\nu(\text{CO})$  bands due to acetaldehyde to the low-frequency region from 1743 to 1684 cm<sup>-1</sup> suggests the formation of a donor–acceptor complex. At 200°C, bands at 1372 and 1634 cm<sup>-1</sup> due to vinyl chloride and bands at 1470 and 1570 cm<sup>-1</sup> characteristic of surface carbonate–carboxylate structures, and an intense band at 1590 cm<sup>-1</sup> due to oligomers appeared in the spectrum. At 300°C, DCE was almost completely converted into products; in this case, the intensities of the absorption bands of vinyl chloride, 1,3-dichloro-2-butene, and acetaldehyde decreased, whereas the intensities of bands due to carbonate–carboxylate structures and oligomers on the surface (1470 and 1590 cm<sup>-1</sup>) increased. At 400°C, only carbonate–carboxylate structures remained on the surface. Upon the adsorption of DCE on  $\gamma$ -Al<sub>2</sub>O<sub>3</sub>, a decrease in the intensities of initial Al–OH groups (bands in the range of 3670–3790 cm<sup>-1</sup>) and the formation of hydrogen-



**Fig. 5.** The time dependence of the relative concentrations of adsorbed DCE and its conversion products on the surface of  $\gamma$ - $\text{Al}_2\text{O}_3$  at 100°C: (1) DCE ( $1431\text{ cm}^{-1}$ ), (2) vinyl chloride ( $1634\text{ cm}^{-1}$ ), (3) 1,3-dichloro-2-butene ( $1652\text{ cm}^{-1}$ ), (4) diene-type oligomers ( $1590\text{ cm}^{-1}$ ), (5) acetaldehyde ( $1684\text{ cm}^{-1}$ ), and (6) carbonate-carboxylates ( $1540\text{ cm}^{-1}$ ).

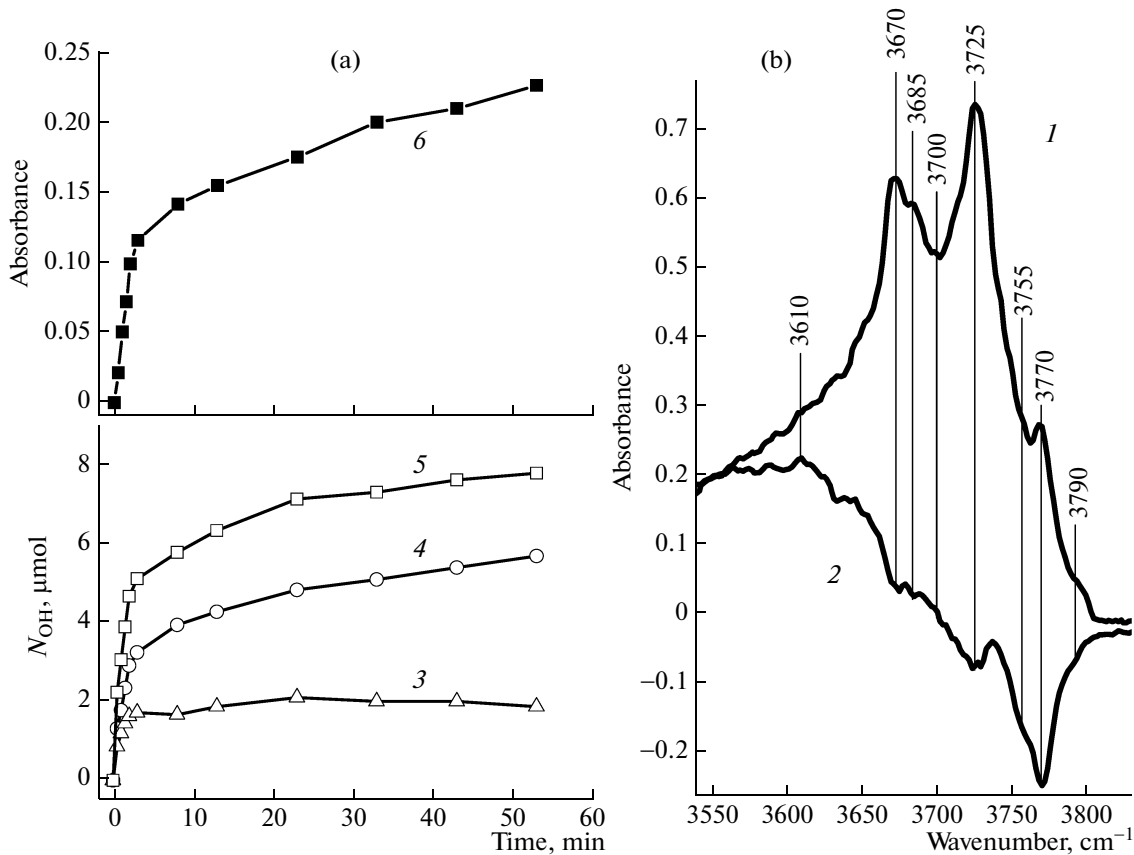
bonded OH groups (a band at  $3570$ – $3610\text{ cm}^{-1}$ ) were observed at all of the temperatures. In the spectra measured upon heating to  $400^\circ\text{C}$ , when the conversion of DCE was complete, a band at  $1630\text{ cm}^{-1}$  due to the deformation vibration of water was absent. On this basis, we can conclude that the band at  $3570$ – $3610\text{ cm}^{-1}$  was due to the interaction of newly formed Al–OH groups with one another rather than water adsorption on Al–OH groups.

Figure 5 shows changes in the concentrations of adsorbed substances on  $\gamma$ - $\text{Al}_2\text{O}_3$  in the course of DCE dehydrochlorination at  $100^\circ\text{C}$ . A maximum DCE adsorption on  $\gamma$ - $\text{Al}_2\text{O}_3$  (Fig. 5, curve 1) was reached only 1.5 min after the onset of the reaction. An increase in the time taken to reach a maximum, as compared with that on the zeolite, was due to the fact that the adsorption of DCE was accompanied by a reaction. An increase in the concentration of 1,3-dichloro-2-butene was observed simultaneously with an increase in the concentration of DCE (curve 3). The concentrations of vinyl chloride (curve 2) and oligomers (curve 4) increased in the course of the entire experiment. Curves 5 and 6 show the kinetics of formation of carbonate–carboxylate structures and acetaldehyde, respectively. The amount of adsorbed acetaldehyde reached a maximum value of 1.6% on an injected DCE basis in the first 3 min and then decreased to 1.3% because of its conversion into carboxylates. The amount of carboxylates became as high as 15% within the measurement time.

Analogously to that for the zeolite, we calculated the rate constants of DCE dehydrochlorination on

alumina. They were  $1 \times 10^{-3}\text{ s}^{-1}$  at the initial portion of curve 1 (Fig. 5) from 2 to 8 min and  $0.17 \times 10^{-3}\text{ s}^{-1}$  over the range of 20–50 min. Evidently, catalyst deactivation occurred in the course of reaction. This was due to the accumulation of coke deposits (oligomers) or the degradation of LASs under the action of HCl. Unfortunately, direct observation of LASs in the course of dehydrochlorination is impossible; however, we can follow the interaction of HCl with the surface using the spectra of OH groups.

The IR spectra of the OH groups of  $\gamma$ - $\text{Al}_2\text{O}_3$  (Fig. 6) before and after DCE injection (curves 1 and 2, respectively) indicate that the intensity of bands due to terminal Al–OH groups ( $3755$ ,  $3770$ , and  $3790\text{ cm}^{-1}$ ) dramatically decreased. The amount of bridging Al–OH groups ( $3670$ ,  $3685$ , and  $3700\text{ cm}^{-1}$ ) changed only slightly. The amount of Al–OH groups characterized by an absorption band at  $3725\text{ cm}^{-1}$  (curve 3) rapidly decreased in the first 2 min and then remained at an almost constant level (in Fig. 6b,  $N$  is the number of removed OH groups). The amount of terminal OH groups (band at  $3770\text{ cm}^{-1}$ , curve 4) after the rapid initial decrease continued to decrease in the course of the entire experiment. The character of the increase in the amount of hydrogen-bonded OH groups appeared upon adsorption ( $3610\text{ cm}^{-1}$ , curve 6) was similar to the character of the decrease in the total amount of terminal and bridging OH groups (curve 5). As can be seen in Fig. 5 (curve 1), 64% ( $8\text{ }\mu\text{mol}$ ) 1,2-dichloroethane was converted into products in 53 min. In this case, HCl was not detected in the gas phase of the cell (at a measurement sensitivity of 1–2% on a basis of



**Fig. 6.** IR spectra of OH groups in  $\gamma$ -Al<sub>2</sub>O<sub>3</sub>. (a) IR spectra of OH groups in (1) initial  $\gamma$ -Al<sub>2</sub>O<sub>3</sub> and (2) 53 min after DCE adsorption at 100°C. (b) Decrease in the amount of OH groups in  $\gamma$ -Al<sub>2</sub>O<sub>3</sub> ( $N_{\text{OH}}$ ) with time: (3, 4) OH groups characterized by absorption bands at (3) 3725 and (4) 3770  $\text{cm}^{-1}$ ; (5) the total amount of terminal and bridging OH groups; (6) band intensity at 3610  $\text{cm}^{-1}$  (for clarity, curves 3–5 are shown as curve 6).

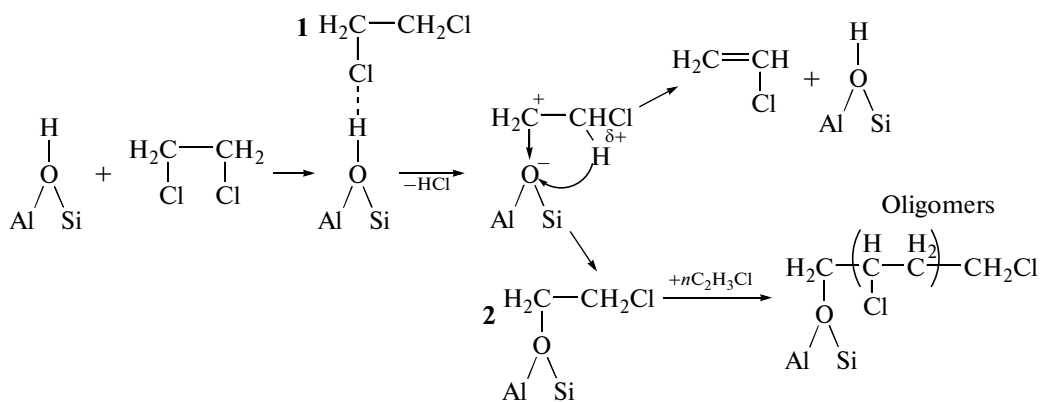
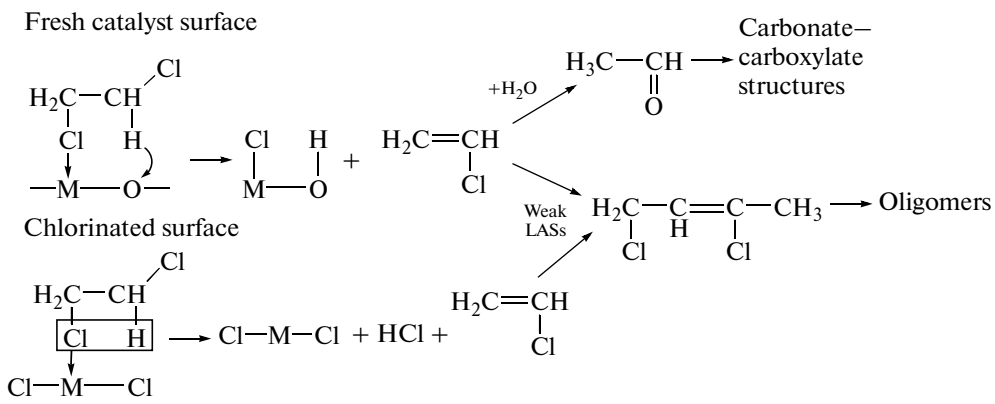
DCE injected into the cell). The amount of disappeared OH groups (8  $\mu\text{mol}$ ) was close to the amount of HCl released upon DCE dehydrochlorination. Consequently, HCl formed in the course of DCE dehydrochlorination reacted with the surface of aluminum oxide to form new OH groups bound to Al—OH groups (a band at 3610  $\text{cm}^{-1}$ ) by hydrogen bonds. The rapid change in the amount of OH groups occurred in the first 8–10 min, which approximately correspond to the initial portion of the kinetic curve of DCE conversion (Fig. 5). It is likely that deactivation at this portion was due to the following reaction: DCE + AlOAl  $\rightarrow$  vinyl chloride + AlCl + AlOH. The subsequent deactivation can be related to the accumulation of oligomers on the surface.

An analysis of the kinetics of DCE conversion demonstrated that deactivation on  $\gamma$ -Al<sub>2</sub>O<sub>3</sub> occurred during the entire measurement time because the  $w/C_{\text{DCE}}$  ratio continuously changed. The formation of vinyl chloride, as well as oligomers and a dimer, occurred in the course of DCE adsorption; therefore, the initial rate constant of dehydrochlorination cannot be measured. It is likely that the initial rate of dehydro-

chlorination is close to the rate of adsorption; that is, its value is  $\sim 10^{-1} \text{ s}^{-1}$ . After 53 min, the rate constant decreased to  $0.13 \times 10^{-3} \text{ s}^{-1}$ . Comparing the initial rate constants of dehydrochlorination on zeolite, where the reaction occurred at LASs and  $\gamma$ -Al<sub>2</sub>O<sub>3</sub>, we can conclude that the leading factor responsible for the activity of LASs is the strength of these sites. At sites with  $Q_{\text{CO}} = 55 \text{ kJ/mol}$  at 100°C on  $\gamma$ -Al<sub>2</sub>O<sub>3</sub>, the rate constant of dehydrochlorination was much higher than that on sites with  $Q_{\text{CO}} = 36 \text{ kJ/mol}$  on zeolite at 200°C.

#### Mechanism of DCE Dehydrochlorination

Based on the results of kinetic studies, we can propose the following reaction schemes for DCE conversion with the participation of LASs and BASs. Two mechanisms of DCE conversion occurred at LASs (Scheme 1). On the surface of a fresh catalyst without contact with DCE, dehydrochlorination occurred at an acid–base pair formed by closely spaced Lewis acid and basic sites. DCE was added to a coordinatively unsaturated metal atom through a chlorine atom; because of this, the C–H bond of the neighboring



$\text{CH}_2\text{Cl}$  group became polarized and hydrogen interacted with the basic site. Next, C–Cl and C–H bonds cleaved to form  $\text{AlCl}$  and OH groups. On  $\gamma\text{-Al}_2\text{O}_3$ , these transformations took place even at room temperature. On a chlorinated surface, that is, under the steady-state conditions of a flow experiment, the dehydrochlorination of DCE also began with the formation of a donor–acceptor bond of the molecule with an LAS through a chlorine atom. As a consequence, the C–Cl became weaker and the C–H bond became polarized; then, an intramolecular transition of hydrogen to the chlorine atom took place to result in the formation of an  $\text{HCl}$  molecule and vinyl chloride. The reaction can occur via this path only at high temperatures. As found by Shalygin et al. [5], dehydrochlorination on  $\gamma\text{-Al}_2\text{O}_3$  occurred at a noticeable rate only at temperatures higher than  $300^\circ\text{C}$ . The resulting vinyl chloride desorbed from the catalyst surface or underwent hydrolysis to acetaldehyde or dimerization to 1,3-dichloro-2-butene at weak LASs. Next, 1,3-dichloro-2-butene underwent oligomerization and acetaldehyde converted into carbonate–carboxylate structures.

Both oligomers and carbonate–carboxylate structures can be responsible for catalyst deactivation. In

this case, the reaction occurred at a maximum rate until sites for the irreversible adsorption of  $\text{HCl}$  occurred on the surface. Thus, at the initial portions of kinetic curves, the conversion of DCE was accompanied by the deactivation of active sites by released  $\text{HCl}$ ; this resulted in similar rates of reaction and deactivation.

Another mechanism occurred on zeolite BASs (Scheme 2). At the first step, DCE formed a hydrogen bond with a BAS through a chlorine atom to give complex 1. At the second step, which is characterized by a high activation energy, complete proton transfer from surface oxygen to a chlorine atom occurred with the formation of  $\text{HCl}$  and an unstable carbocation. Next, the carbocation can eliminate a proton from the neighboring  $\text{CH}_2\text{Cl}$  group with the formation of vinyl chloride and the regeneration of a BAS or interact with  $\text{O}^-$  through the  $\text{CH}_2$  group to form alkoxide structure 2, which initiates the oligomerization of vinyl chloride.

Note that the oligomerization of vinyl chloride on BASs, as distinct from LASs, occurred without the intermediate formation of 1,3-dichloro-2-butene. The oligomerization of ethylene and propylene on zeolite HZSM-5 occurred in a similar manner [10].

The appearance of dimers was noted only at an elevated temperature as a result of the cracking of oligomer chains [10]. The formation of an amount of 1,3-dichloro-2-butene, which was observed upon DCE adsorption on zeolite HZSM-5 at 300–400°C (Fig. 1), can also be due to the cracking of chlorine-containing oligomers.

Thus, we found that the dehydrochlorination on BASs occurred much more slowly than that at LASs. This was likely due to the fact that the dehydrochlorination on BASs occurred by a carbenium ion mechanism with large energy consumption. Two mechanisms were found for the dehydrochlorination at LASs. On a fresh surface of aluminum oxide, the dehydrochlorination occurred at an acid–base pair at a high rate because of a decrease in the endothermicity of DCE dehydrochlorination reaction because of the chemisorption of HCl. After the termination of HCl absorption, dehydrochlorination by this mechanism stopped. On a chlorinated surface of aluminum oxide, the dehydrochlorination occurred more slowly than on the fresh surface; this was due to a change in the nature of a rate-limiting step. On the chlorinated surface, vinyl chloride appeared after the formation of an H–Cl bond, and it appeared on the fresh surface after the formation of an H–O bond, which is much stronger than the H–Cl bond, as is well known.

## REFERENCES

1. Lakshmanan, A., Rooney, W.C., and Biegler, L.T., *Comput. Chem. Eng.*, 1999, no. 23, p. 479.
2. Uvarova, E.B., Kustov, L.M., Lishchiner, I.I., Malova, O.V., and Kazansky, V.B., *Stud. Surf. Sci. Catal.*, 1997, vol. 105, no. 2, p. 1243.
3. Feijen-Jeurissen, M.M.R., Jorna, J.J., Nieuwenhuys, B.E., Sinquin, G., Petit, C., and Hindermann, J.-P., *Catal. Today*, 1999, vol. 54, no. 1, p. 65.
4. Rivas, B., Lopez-Fonseca, R., Gonzalez-Velasco, J.R., and Gutierrez-Ortiz, J.I., *J. Mol. Catal. A: Chem.*, 2007, vol. 278, nos. 1–2, p. 181.
5. Shalygin, A.S., Koval', L.M., Malysheva, L.V., Kotsarenko, N.S., and Paukshtis, E.A., *Khim. Interes. Ust. Razv.*, 2009, vol. 17, no. 4, p. 423.
6. Makarova, M.A., Paukshtis, E.A., Thomas, J.M., Williams, C., and Zamaraev, K.L., *J. Catal.*, 1994, vol. 149, no. 1, p. 36.
7. Paukshtis, E.A., *Infrakrasnaya spektroskopiya v geterogennom kislotno-osnovnom katalize* (Infrared Spectroscopy in Heterogeneous Acid–Base Catalysis), Novosibirsk: Nauka, 1992.
8. *NIST Chemistry Webbook*, <http://webbook.nist.gov/chemistry>.
9. Davydov, A.A., *Molecular Spectroscopy of Oxide Catalyst Surfaces*, Chichester: Wiley, 2003.
10. Medin, A.S., Borovkov, V.Yu., and Kazanskii, V.B., *Kinet. Katal.*, 1989, vol. 30, no. 1, p. 177.